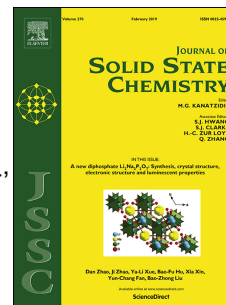


Journal Pre-proof

Heat capacity and magnetocaloric effect in the zircon and scheelite phases of $RCrO_4$,
 $R = Tb, Er, Ho$

E. Palacios, M. Castro, J. Romero de Paz, J.M. Gallardo-Amores, R. Sáez-Puche



PII: S0022-4596(22)00481-9

DOI: <https://doi.org/10.1016/j.jssc.2022.123356>

Reference: YJSSC 123356

To appear in: *Journal of Solid State Chemistry*

Received Date: 30 March 2022

Revised Date: 14 June 2022

Accepted Date: 19 June 2022

Please cite this article as: E. Palacios, M. Castro, J. Romero de Paz, J.M. Gallardo-Amores, R. Sáez-Puche, Heat capacity and magnetocaloric effect in the zircon and scheelite phases of $RCrO_4$, $R = Tb, Er, Ho$, *Journal of Solid State Chemistry* (2022), doi: <https://doi.org/10.1016/j.jssc.2022.123356>.

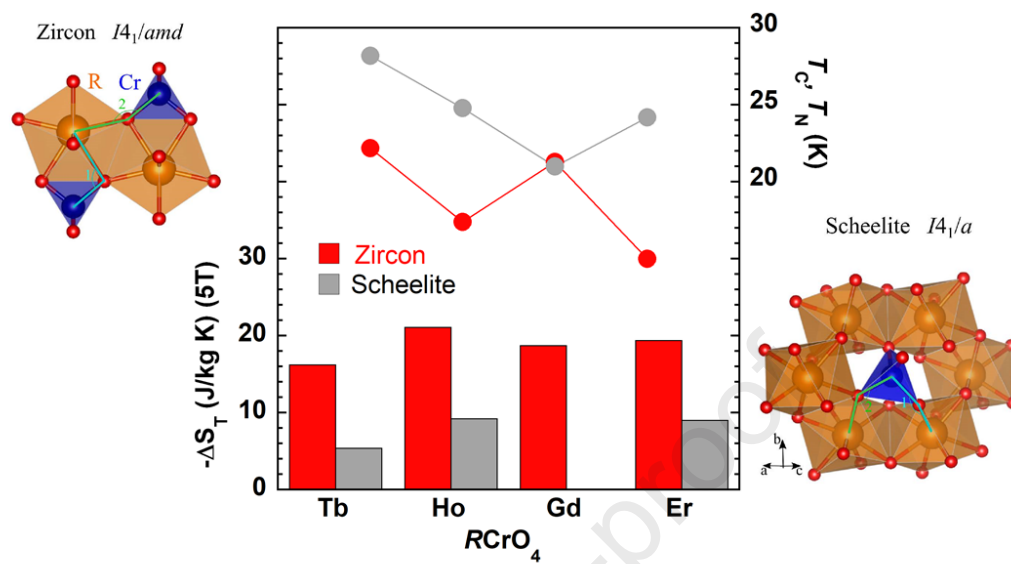
This is a PDF file of an article that has undergone enhancements after acceptance, such as the addition of a cover page and metadata, and formatting for readability, but it is not yet the definitive version of record. This version will undergo additional copyediting, typesetting and review before it is published in its final form, but we are providing this version to give early visibility of the article. Please note that, during the production process, errors may be discovered which could affect the content, and all legal disclaimers that apply to the journal pertain.

© 2022 Published by Elsevier Inc.

Credit Author Statement

Elias Palacios. Conceptualization. Methodology. Investigation. Magnetocaloric effect. Writing - Original Draft. **Miguel Castro.** Investigation. Heat Capacity. Writing - Review & Editing. **Julio Romero de Paz.** Investigation. Preparation of zircons. Writing - Review & Editing. **José Manuel Gallardo-Amores.** Investigation. High pressure. Preparation of scheelites. Writing - Review & Editing. **Regino Sáez-Puche.** Conceptualization. Methodology. Investigation. Magnetization measurements. Writing - Review & Editing.

Journal Pre-proof



Heat capacity and magnetocaloric effect in the zircon and scheelite phases of $R\text{CrO}_4$, $R = \text{Tb}, \text{Er}, \text{Ho}$

E. Palacios^{a,b}, M. Castro^{b,c}, J. Romero de Paz^d, J. M. Gallardo-Amores^d,
R. Sáez-Puche^d

^a*Departamento de Física de la Materia Condensada, Universidad de Zaragoza, 50009 Zaragoza, Spain*

^b*Instituto de Nanociencia y Materiales de Aragón (INMA), CSIC–Universidad de Zaragoza, 50009 Zaragoza, Spain*

^c*Departamento de Ciencia y Tecnología de Materiales y Fluidos, Universidad de Zaragoza, 50018 Zaragoza, Spain*

^d*Departamento de Química Inorgánica, Universidad Complutense de Madrid, 28040 Madrid, Spain*

Abstract

We present here new magnetization and heat capacity data under magnetic field and direct measurements of the magnetocaloric effect (MCE) in the zircon and the new scheelite phases of $R\text{CrO}_4$ ($R = \text{Tb}, \text{Er}, \text{Ho}$) from 5 K to 100 K, for magnetic fields B from 0 to 9 T. Zircons have a high MCE near their Curie point, $T_C \simeq 20$ K, reaching maximum isothermal entropy increments, $|\Delta S_T| = 21, 19.4,$ and $16.2 \text{ J kg}^{-1}\text{K}^{-1}$ for $\text{HoCrO}_4, \text{ErCrO}_4,$ and TbCrO_4 , respectively, for an external field of 5 T. TbCrO_4 has another anomaly near $T_D = 60$ K associated to a Jahn-Teller transition from the tetragonal zircon structure to an orthorhombic phase. Scheelites are antiferromagnetic with $T_N \simeq 25$ K. In the Tb scheelite the rare earth is strongly coupled to Cr^{5+} and the MCE exhibits the typical features of an antiferromagnet, *i.e.* a sort of Curie-Weiss behavior above T_N and a sudden drop to small or even inverse values below. In the Er and Ho scheelites the R^{3+} - Cr^{5+} exchange coupling is very weak and the R^{3+} ion behaves independently of the Cr^{5+} . As a striking consequence the MCE is quite stronger well below T_N .

Keywords: Polymorphism of $R\text{CrO}_4$ oxides, Magnetic measurements, Heat capacity and entropy, Magnetocaloric effect

Email address: elias@unizar.es (E. Palacios)

1. Introduction

Refrigeration by demagnetization of a material with strong magnetocaloric effect (MCE) is a procedure used since the 1930's to reach temperatures below 1 K [1]. The method was intended for reaching the lowest possible temperatures, with scientific purposes. Therefore, in that time paramagnetic salts were used. These are composed by ions of high magnetic moment separated by many non magnetic ones preventing ordering by magnetic dipolar interaction, which allowed to cool down to 40 mK by routine, in a single shot. Today there are other procedures of refrigeration, but it turns out that the old demagnetization method is thermodynamically very efficient. Moreover, refrigeration at temperatures of the boiling points of helium, hydrogen or natural gas overtakes the pure scientific research by a large amount, when liquid helium is currently used in many scenarios, hydrogen is proposed as a clean energy vector, and natural gas is a fuel reducing considerably the emission of CO₂ to the atmosphere, with respect to other usual hydrocarbons. A review of materials and systems for magnetic refrigeration at cryogenic temperatures is [2], where the full section of the volume is devoted to the subject. A more recent review is [3].

The ideal material to use the MCE for refrigeration above 1 K would be composed of atoms with high spin, high density of magnetic moments, low anisotropy, and weak exchange interactions. This is the case of the previously studied zircon phase of GdCrO₄ [4, 5, 6] where the partial polarization of the Gd³⁺ ions confers to this compound a high MCE over a wide temperature range, with $|\Delta S_T| > 20 \text{ J kg}^{-1}\text{K}^{-1}$ between 5 K and 35 K and a maximum of $29 \text{ J kg}^{-1}\text{K}^{-1}$ at 22 K, in both cases for a field increment from zero to 9 T. The gadolinium compound is the most evident case among the zircons $R\text{CrO}_4$ ($R = \text{rare-earth atom}$) because of the virtually isotropic behavior of Gd³⁺, in the temperature range of this work, but other rare earths can be explored. In this sense, it has been reported that other zircons $R\text{CrO}_4$ ($R = \text{Ho and Dy}$) show also large values of the magnetocaloric parameters that make of these oxides potential refrigerant materials [7]. Moreover, recently the scheelite polymorphs (space group, *s. g.* $I4_1/a$) have been synthesized at high pressure from the zircon phases for most R elements. These scheelite forms are quenchable after releasing the pressure [6, 8, 9, 10, 11, 12, 13, 14, 15, 16, 17].

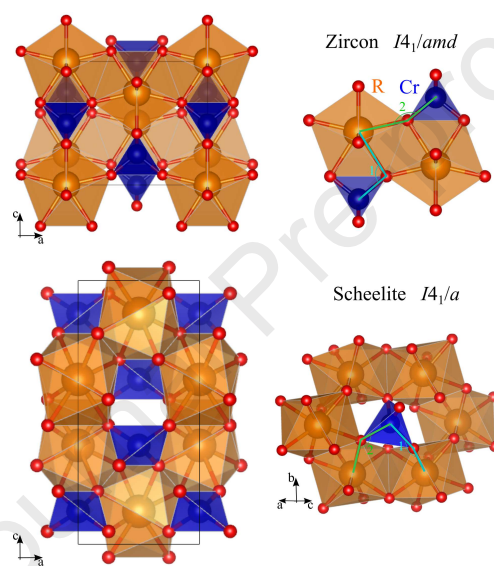


Figure 1: Left side: Perspective view of the zircon and scheelite-type structures showing the edge sharing chains of RO_8 bispindenoids. Blue: Cr^{5+} , red: O^{2-} , orange: R^{3+} . Right side: Two possible R - Cr exchange pathways 1 and 2 in both structures, showing the very different R - O - Cr angles that determine the sign of the interaction.

Most of the zircon-type $R\text{CrO}_4$ oxides behave as ferromagnetic (FM), while the scheelite polymorphs are made of ferromagnetic layers, perpendicular to the c -axis, coupled antiferromagnetically (AFM). The change in the sign of the magnetic interaction can be explained by considering the changes in the bond angles of Cr-O- R pathways through which the superexchange interactions take place in these two structural types, see Fig. 1. In the case of the zircon polymorphs the pathway 1 (Fig. 1) with a bond angle near of 90° ($94.8(2)^\circ$ for TbCrO_4 is a typical example) accounts for the observed FM interaction, while for the scheelite polymorphs the corner sharing between the $[\text{RO}_8]$ and $[\text{CrO}_4]$ polyhedra significantly increases that Cr-O- R angle (to $132.3(3)^\circ$ for TbCrO_4) and with it the type of interaction changes from FM to AFM. In addition to the fundamental physical and chemical properties, the following features make these $R\text{CrO}_4$ oxides suitable for potential refrigerant in comparison with other rare earth transition metal oxides. First, a large magnetic moment, typical of many rare earth ions, makes easier the polarization by a moderate external magnetic field. Second, for some rare earths the crystal field (CF) favor the thermal population of many magnetic states (*i.e.* random distribution of the magnetic moment directions above T_N or T_C but still at low temperatures) at zero field. Third, the exchange interaction with the $3d$ -ion, usually much higher than $R-R$ exchange interaction, provides an internal field increasing the polarization below the ordering temperature.

The Cr^{5+} ion plays an important role as promoter of the interactions in the rare earth sublattice increasing the ordering temperatures by one order of magnitude in comparison with the analogous $R\text{XO}_4$ ($X = \text{P}, \text{As}, \text{V}$) where X is a diamagnetic element [18, 19]. The order temperatures in these compounds are well below 5 K, indicating that the direct $R-R$ interaction is much weaker than $R\text{-Cr}$ or Cr-Cr . On the other hand, the lower T_C in the Cr-zircons where R is not magnetic (e.g. YCrO_4 [9] or LuCrO_4 [8]) indicates that the $R\text{-Cr}$ interaction is relevant and enhances the FM coupling. Additionally, a ferroelectric transition near 100 K has been reported in $R\text{CrO}_4$ ($R = \text{Y}, \text{Gd}, \text{Ho}, \text{Sm}$), related to a distortion of the CrO_4^{3-} tetrahedra [20]. This fact opens the possibility of changing the exchange interactions, thus a magnetoelectric effect.

The structural and magnetic properties of the zircon and scheelite polymorphs of $R\text{CrO}_4$ ($R = \text{Tb}, \text{Er}, \text{Ho}$) have been discussed in a previous series of papers [8, 9, 11, 12, 13, 14, 15, 16, 21, 22]. The heat capacity was studied at zero magnetic field and for the scheelite TbCrO_4 also at 3 T and 8 T [14].

This work is essentially focused on the MCE of both polymorphs of $R\text{CrO}_4$ ($R = \text{Er, Ho, Tb}$) oxides, by studying the isothermal entropy change, ΔS_T , associated to the applied magnetic field change $\Delta B = B - 0$ (see section 2.3.1). Thus, ΔS_T is obtained from isothermal magnetization, from heat capacity data at several magnetic fields and by direct measurements of the heat released/absorbed on isothermal magnetization/demagnetization. The heat capacity data are analysed in relation with the CF splitting of the ground level of each rare earth ion. A possible Dzialozhinsky-Moriya interaction in scheelites has a too small influence in the MCE. Although it is never explicitly stated we will assume a simple Heisenberg interaction hamiltonian, as the anisotropy comes mainly from the CF at the rare earth ion site.

2. Experimental details

2.1. Sample preparation

Zircon-type $R\text{CrO}_4$ powder samples were prepared by heating the stoichiometric amounts of $\text{Cr}(\text{NO}_3)_3 \cdot 9 \text{H}_2\text{O}$ and $R(\text{NO}_3)_3 \cdot 6 \text{H}_2\text{O}$ in an oxygen flow according to the following thermal process: 30 min at 433 K, 30 min at 473 K and 10-12 h at 853 K. Scheelite-type $R\text{CrO}_4$ powder samples were obtained in a belt type press from the corresponding zircon-type $R\text{CrO}_4$ under a high pressure of 40 kbar and 833 K for 30-40 min [12, 14, 23]. For both polymorphs, the X-ray powder diffraction patterns obtained confirmed the respective structures and purity.

2.2. Magnetization measurements

New isothermal DC magnetization M data were collected using a Quantum Design Physical Property Measurement System (PPMS), from 2 K to 60 K and for applied magnetic fields B up to 9 T. These measurements were used to deduce the MCE. Only the M -data for the scheelite TbCrO_4 are shown (Fig. 7), since most of results have been discussed in previous works. We give the M -data in a double scale, since in μ_B/fu they are more directly related to the atomic properties than in emu/g. The DC magnetic susceptibility, χ , has been deduced as $\chi = M/B$ for low field data. The AC susceptibility has been taken from previous works.

2.3. Heat capacity and entropy

For the determination of the heat capacity, $C_{p,B}$, the usual relaxation procedure is used in a PPMS at constant magnetic fields from 0 to 9 T and

very low pressure, using a pellet of pressed powder. The accuracy is better than 5% between 2 K and 50 K. To determine the phonon contribution of the zircon phases the heat capacity of LuCrO₄ [10] has been used, where Lu³⁺ is not magnetic and Cr⁵⁺ orders at the low $T_N = 9.2$ K, allowing to extrapolate the experimental higher temperature data to $T \rightarrow 0$ by a Debye function. For other zircons an empirical corresponding states law was used as an estimation of the phonon contribution, *i.e.* $C_{ph} \simeq C_{ph}(\text{LuCrO}_4, T/fs)$ using a proper scale factor $fs \simeq 1$. This estimation reproduces well the heat capacity of other zircons like YCrO₄ [10] and GdVO₄ [24] at temperatures where the magnetic contribution is negligible. These compounds have no contribution of the crystal- field either. For scheelites a corresponding states law has been applied to the very precise, reliable and recent experimental data of LaNbO₄, by adiabatic calorimetry [25]. This law reproduces acceptably the experimental heat capacity of YVO₄, despite of the very different atomic masses in both compounds.

To estimate the contribution of the thermal population of the CF levels in zircons, the isostructural RVO₄ compounds [18] have been used, when the CF is essentially produced by the charge of O²⁻ in all cases. For the ErCrO₄ sheelite, the levels of Er-doped scheelites AMoO₄ ($A = \text{Ca, Sr, Pb}$) [26] have been assumed. Lacking any direct determination of the CF splitting in other scheelite-oxides, the data of the RLiF₄ [27, 28, 29, 30, 31, 32] have been taken. Because of the higher O²⁻ charge *vs.* F⁻, the CF splitting of the ground free ion manifold in the fluorides must be quite smaller than in the orthochromates, but we assume that at least the splitting scheme is the same in both compounds for every R .

The entropies have been determined by the thermodynamic relation

$$S(T, B) = S(T_0, B) + \int_{T_0}^T \frac{C_{p,B} dT}{T} \quad (1)$$

Here $T_0 = 0$ is taken when a clear extrapolation of the experimental data to $T \rightarrow 0$ is possible (*e.g.* for a high applied field), assuming $S(0, B) = 0$. Otherwise another different temperature $T_0 \gg 0$ is taken using the experimental difference $S(T_0, B_2) - S(T_0, B_1)$, obtained from magnetocaloric measurements, for setting $S(T_0, B_2)$, knowing $S(T_0, B_1)$. The molar heat capacity and entropy are given always in units of the gas constant R , that should be not confused with the symbol for a rare earth. In these units they are directly related to atomic properties (*e. g.* the entropy is an experimental

measurement of the logarithm of the number of thermally accessible states, per chemical unit). ΔS_T (MCE) is given in double scale, per unit of mass, and molar.

2.3.1. Magnetocaloric effect

145 The magnetocaloric effect is characterized by the isothermal entropy change, ΔS_T , or the adiabatic temperature change, ΔT_{ad} , for a magnetic field variation $\Delta B = B - 0$. ΔS_T has been obtained at least in two of the three following ways:

- 1) Directly, by the procedure described in [33].
- 150 2) From isothermal magnetization data, M , via the well-known Maxwell relation

$$\left(\frac{\partial S}{\partial B}\right)_T = \left(\frac{\partial M}{\partial T}\right)_B \Rightarrow$$

$$\Delta S_T \equiv S(T, B) - S(T, 0) = \int_0^B \left(\frac{\partial M}{\partial T}\right)_B dB \quad (2)$$

- 3) From heat capacity data at several constant fields, via the deduced entropies, $\Delta S_T = S(T, B) - S(T, 0)$.

Usually these three methods are complementary. The values deduced
 155 from M are not always precise or even correct. The entropies deduced from $C_{p,B}$ frequently involve a not well determined constant and the direct determinations are only possible in a narrower temperature range. The initial field is always assumed zero throughout this work, and we write always B for ΔB to simplify the notation. It should be noted that the results from
 160 M should be slightly higher than from $C_{p,B}$ or directly measured, due to the different demagnetization factor of the samples used for each experiment, when $B = \mu_0 H$ is always the external field.

3. Results and discussion

3.1. Heat capacity of zircons

165 3.1.1. $TbCrO_4$

The heat capacity of the zircon $TbCrO_4$ (Fig. 2) at zero field shows a λ -peak at $T_C = 22.2(1)$ K in agreement with other determinations [34, 9]. This anomaly rounds off and its maximum moves to higher temperature on application of a weak external magnetic field indicating a FM ordering, like

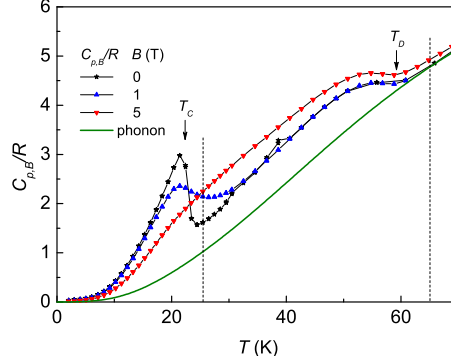


Figure 2: Heat capacity of the zircon phase of TbCrO_4 . Continuous line: Estimation of the phonon contribution as explained in the experimental section. Vertical lines indicate the temperatures at which the entropy is given.

170 most of zircons. There is another round anomaly starting near $T_D = 60$ K and downwards. We ascribe this anomaly to a co-operative Jahn-Teller (JT) distortion (very usual also in other rare earth zircons like RXO_4 with $R = \text{Tb}$, Dy, Tm and $X = \text{V}$, As or P) from the room temperature (RT) tetragonal zircon structure to an orthorhombic phase which has been described with the *s. g.* $F222$ [34] and more recently with $Fddd$ [8]. Differently of other
 175 Tb zircons (*e.g.* TbVO_4 [35]) this transition does not have the typical λ shape of the second-order transitions. In our opinion that is due to the stress distribution in the pellet used for $C_{p,B}$ measurements, since the JT transition is very sensitive to stress [36]. In contrast, the anomaly is insensitive to a
 180 magnetic field lower than 5 T. At zero field, the magnetic anomaly in C_p occurs well below T_D . The much higher T_D with respect to that for TbVO_4 would be related to a stronger electron-phonon coupling in the Cr compound producing a wider splitting of the ground quasi-quartet of Tb^{3+} as explained in [36].

185 The entropy of both anomalies together (*i.e.* the experimental entropy at zero field minus the estimated normal phonon contribution), at 65 K is $S_{anom}/R = 2.13$. To understand this value, let us consider the well known isostructural TbVO_4 . It has a JT distortion at $T_D = 33.1$ K [35, 18]. In the tetragonal phase of TbVO_4 the lowest crystal-field levels of Tb^{3+} are one singlet (ground state), one doublet at $8.6 \text{ cm}^{-1} = 12.4$ K (the factor
 190 $E(\text{K})/E(\text{cm}^{-1}) = 1.439 \text{ K/cm}^{-1}$ will be implicitly invoked throughout this

paper), and one singlet at 22.9 cm^{-1} . Next level is at 91.5 cm^{-1} , clearly too high in energy to be thermally populated at T_D . The total theoretical anomalous entropy, considering a contribution of Cr^{5+} as $\ln(2)$, would be
 195 $S_{anom}/R = \ln(2) + \ln(4) = \ln(8) = 2.08$, very close to the observed value. However in TbCrO_4 the anomaly in C_p at zero field occurs below 60 K. Therefore the thermal occupation of the next excited levels at 60 K would explain the observed excess of anomalous entropy above $\ln(8)$. Now let us consider the entropy at 25.5 K, just above the λ -peak. Subtracting the
 200 phonon contribution it gives $S_{anom}/R = 1.28$, slightly below $2\ln(2) = 1.39$, which can be interpreted as the magnetic contribution of Cr^{5+} plus a full thermal population of the ground CF doublet of Tb^{3+} in the orthorhombic phase.

Within this interpretation, it is to be remarked that M does not reach
 205 saturation even at 2 K for 9 T, when $M = 135 \text{ emu/g} = 6.64 \mu_B/fu$, while the moments determined by neutron diffraction [9] are $\mu(\text{Tb}^{3+}) = 7.62(8) \mu_B$, $\mu(\text{Cr}^{5+}) = 0.96(3) \mu_B$, giving a saturation magnetization $M_s = 8.6(1) \mu_B/fu$, much higher than observed. The explanation is the strong anisotropy of Tb and the random orientation of the crystallites in a powder sample, when only
 210 the parallel component of the field to the easy direction produces a relevant polarization effect.

3.1.2. HoCrO_4

The lowest lying CF levels of Ho^{3+} in HoVO_4 are a non magnetic singlet ($E_0 \equiv 0$), with $\langle J_z \rangle = 0$, a doublet at $E_1 = 19.5 \text{ cm}^{-1}$, with $J_z \simeq \pm 1$, a
 215 singlet at $E_2 = 43.2 \text{ cm}^{-1}$, with $\langle J_z \rangle = 0$ and a doublet at $E_3 = 44.4 \text{ cm}^{-1}$ with predominance of the states with $J_z = \pm 1$ [37]. Next level is more than 100 cm^{-1} above the ground level but the high $J_z = \pm 7$ make it reachable on application of a strong external magnetic field. Ho^{3+} has no moment for zero field but the relatively near excited doublet produces magnetic polarization
 220 by moderate magnetic fields. For a magnetic field in the ab -plane, the behavior is as van Vleck paramagnet with a large susceptibility. We can assume small changes of the crystal-field levels on going to HoCrO_4 . Therefore, at first, a Schottky anomaly in the zero-field heat capacity (Fig. 3) with maximum near 13 K is expected, due to the thermal occupation of the CF levels,
 225 in addition to the magnetic contribution of Cr^{5+} . This latter contribution is related to a peak at $T_C = 17.4(2) \text{ K}$ which hide somewhat the Schottky anomaly.

The peak becomes a round anomaly under a small field of 1 T, therefore

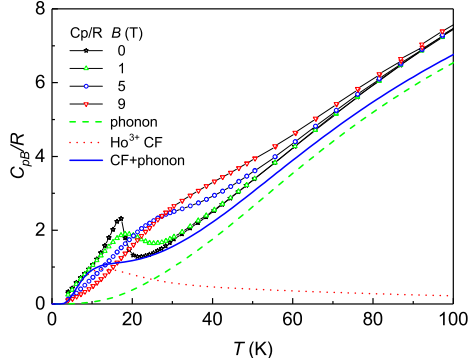


Figure 3: Heat capacity of the zircon phase of HoCrO_4 under several applied magnetic fields. Dashed green line: Estimation of the phonon contribution. Dotted red line: Contribution of the first two crystal-field levels of Ho^{3+} . Solid blue line: sum of phonon and crystal-field contributions.

it is due to the FM ordering of the Cr^{5+} ions, as also deduced from magnetic susceptibility [12]. The magnetic entropy just above the peak (*e. g.* at 26.3 K), where the magnetic contribution of the Cr^{5+} ions should be $S_m/R = \ln(2)$, is actually $S(26.3 \text{ K})/R = 2.31$. It turns out that the sum of the magnetic part, plus the phonon contribution, $S_{ph}/R = 0.28$, plus that of the CF levels, $S_{CF}/R = 1.55$, make a total of $S/R = 2.52$. The value is near that calculated, and most probably the difference is due to an imprecise estimation of the CF levels in HoCrO_4 , taken from HoVO_4 . In any case the heat capacity at zero field can be semiquantitatively explained by the sum of the phonon plus magnetic plus CF contributions at low temperature.

3.2. Heat capacity of scheelites

3.2.1. HoCrO_4

This compound orders antiferromagnetically as reported from χ -data [12]. However this reference gives 7.6 K as Néel temperature, although the present heat capacity data shows a very clear λ -anomaly with the sharp maximum at $T_N = 24.8(2)$ K (Fig. 4). If the maximum in χ is associated to weak-ferromagnetism is to study.

The CF of Ho^{3+} in LiF-scheelites has been studied by several techniques. A recent direct determination of the CF levels by inelastic neutron scattering in HoLiF_4 is given in [32]. The ground manifold of the free ion Ho^{3+} , 5I_8 , splits into four doublets and nine singlets.

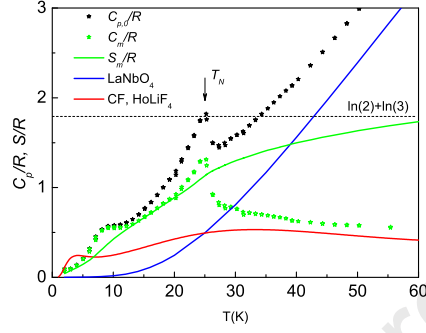


Figure 4: Black symbols: Heat capacity of HoCrO_4 (scheelite) at zero field. Blue line: heat capacity of LaNbO_4 , taken as phonon contribution. Green symbols: Magnetic heat capacity at zero field, C_m , deduced as the experimental data minus the phonon contribution. Red line: Contribution of the crystal-field levels of Ho in HoLiF_4 , after [28], for comparison. Green line: Magnetic entropy.

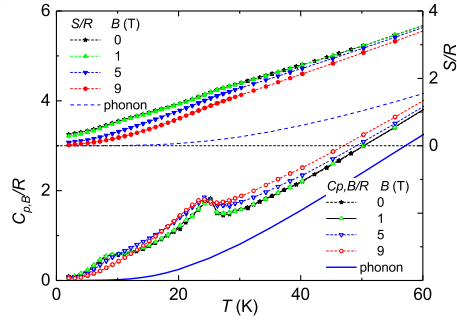


Figure 5: Heat capacity under applied magnetic field (left side scale) and entropy (right side scale) of the scheelite phase of HoCrO_4 .

250 In the scheelite HoCrO_4 , Ho^{3+} is expected to be under a more intense CF
 than in HoLiF_4 . Moreover in the Cr-scheelite the Cr-Ho exchange, similarly
 to a staggered magnetic field, polarizes the Ho^{3+} ions, especially the ground
 doublet, mainly made of $|J_z\rangle = |\pm 7\rangle$ states, below T_N , when the Cr^{5+}
 255 orders. The heat capacity has a bump with maximum at 8 K that can be
 assigned to the thermal occupation of the lowest three CF levels. The phonon
 contribution is estimated as the heat capacity of LaNbO_4 (*i.e.* $fs = 1$). The
 magnetic contribution is deduced by subtraction of last two data sets. For
 comparison, the calculated contribution for the CF levels of Ho^{3+} in HoLiF_4
 is included. The CF levels cannot be deduced from heat capacity, since a
 260 fitting would be ill conditioned, but it is clear than the excess with respect
 to LaNbO_4 is due to the thermal population of the CF levels well above
 T_N (*i.e.* say above 40 K), and to a combination of that and the magnetic
 contribution of Cr^{5+} below this temperature. In this range only the first
 three CF levels (one doublet and one singlet) are significantly populated and
 265 the entropy clearly tends to the theoretical upper limit $S_m(T \rightarrow \infty)/R =$
 $\ln(2) + \ln(3) = 1.79$, before the thermal occupation of higher CF levels will
 become relevant. The bump near 8 K can be related to the observed increase
 in susceptibility [12]. It would be due to two combined effects. First, a larger
 energy difference between the ground doublet and the first excited CF level
 270 in HoCrO_4 . Second, the splitting of the ground doublet by the exchange with
 Cr^{5+} , which apparently is not intense enough to do it at T_N .

Under a weak or moderate external magnetic field of 1 T, the heat ca-
 pacity does not change substantially (Fig. 5), as correspond to an antifer-
 romagnet. For a field of 5 T or stronger the λ -anomaly change slightly, the
 275 maximum becoming more round and shifting to lower temperatures. Appar-
 ently, the spin-flop field of Cr^{5+} would above 9 T. Contrarily the bump near
 8 K shifts to higher temperatures for a field of 5 T or stronger. This fact can
 be understood if such external field is higher than the spin-flip value for the
 staggered polarizing field produced by Cr^{5+} .

280 3.2.2. ErCrO_4

This phase shows similar features to the Ho scheelite, although the CF
 splitting scheme of Er^{3+} is quite different. A peak in the heat capacity at
 $T_N = 24.2$ K (Fig. 6) indicates an AF ordering below this temperature,
 which we assign to the Cr^{5+} atoms, with a small contribution of the Er^{3+}
 285 as discussed in section 3.4. The crystal-field levels of Er^{3+} -doped AMoO_4
 ($A = \text{Ca}, \text{Sr}, \text{Pb}$) scheelites have been deduced from the EPR data [26].

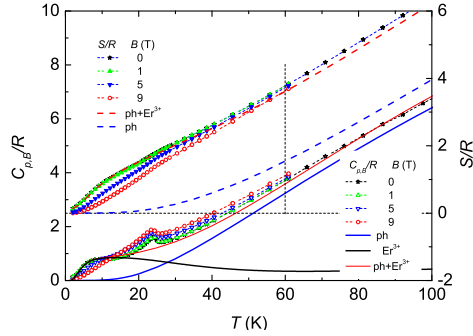


Figure 6: Heat capacity (open symbols, left side scale) and entropy (solid symbols, right side scale) of the scheelite phase of ErCrO_4 . Lines: solid, C_p/R dashed, S/R . Blue line: phonon contribution estimated by corresponding states from LaNbO_4 with $f_s = 1.00$. Black line: Contribution of Er^{3+} as deduced from the crystal-field levels given in the text. Red line: sum of phonon and Er^{3+} contributions.

The ground free-ion manifold $^4I_{15/2}$ splits into 8 Kramers doublets under the local D_{2d} symmetry. In these compounds the spectrum consist of a ground doublet, two doublets at almost the same energy between 23 and 45 cm^{-1} , depending on the compound, a fourth doublet near 50-65 cm^{-1} and the last four doublets above 245 cm^{-1} . In ErLiF_4 the splittings are similar but the second pair of doublets lies at 18 and 20 cm^{-1} [29]. Therefore only the position of the second and the third doublet change substantially from one compound to another. In addition to this, in ErCrO_4 , the effective field produced by the ordered Cr^{5+} ions splits each doublet. For ErCrO_4 , a simplified choice from the data for ErLiF_4 is considered based on: 1) In the range 0-50 K practically only the first four doublets contribute. 2) The exchange with the Cr^{5+} ion would split each doublet. We adjust only the splitting of the ground doublet and keep approximately the same values for the next two doublets. 3) Upper levels practically do not contribute and we take the same values as for ErLiO_4 . That is, we take the energy levels, in kelvin, as -7, 7, 20, 35, 50, 70, 89, 343, 404, 445, 494. The first 6 levels are singlets (split by the exchange with Cr^{5+}) and the last 5 levels are double degenerate (the exchange splitting is neglected).

This estimation is somewhat arbitrary, but there are some unambiguous effects. First, at zero external field, the Schottky-like anomaly with maximum near 10 K is essentially due to the thermal occupation of the first excited

states of Er^{3+} . Second, the low temperature tail of the anomaly cannot be explained without considering the splitting of the ground doublet by the effective exchange field produced by Cr^{5+} . Third, this exchange field is much weaker than in zircons and the polarization of the ground doublet (most probably all doublets) is negligible at T_N or above. Fourth, an external field up to 9 T does not change the peak at $T_N = 24.1(2)$ K, due entirely to the Cr^{5+} ions. That means that the spin-flop field for the Cr^{5+} ions is quite higher than this value, as usual dealing with $3d$ transition metals.

Considering the splitting of the ground doublet, $\Delta E_0 = 14$ K, and the experimental magnetic moment of Er^{3+} at very low temperature [23], $\mu(\text{Er}) = 5.1 \mu_B$, an effective staggered exchange field, $B_{ex} \simeq \Delta E_0 / (2\mu(\text{Er})) = 2$ T, is estimated. At very low temperature (*e. g.* at 2 K) an external field above this value, applied along the easy direction would flip the Er^{3+} moments aligning along the external field. The shoulder in $C_{p,B}$ with maximum near 10 K does not change with applied magnetic fields of 1 T or less (Fig. 6). For high fields the maximum moves to higher temperatures. This change of behavior seems due to a spin-flip transition occurring in the Er sublattice for a field near 1.2 T, as evidenced by a sudden slope change in the magnetization data against field at 2 K [23]. It should be considered that in a powder sample the change is gradual. Therefore the maximum magnetization, measured only up to 5 T, seems compatible with a moment of $5.1 \mu_B$.

After subtraction of the phonon contribution the entropy at zero field and $T \simeq 60$ K is $(S - S_{ph})/R = 2.25$. The entropy of Cr^{5+} is surely very close to $\ln(2) = 0.693$, which leaves $1.55 = \ln(4.7)$ for Er^{3+} , which compares with the theoretical estimation $1.38 = \ln(4)$. Assuming a minor contribution of the upper doublets, it is clearly the contribution of the first two doublets, taken at 0 and 27.5 K, since well above T_N no splitting of the doublets is expected.

3.2.3. TbCrO_4

As explained below, Tb scheelite is also AFM but behaves quite differently to Er and Ho ones. In the isostructural TbLiF_4 the lowest free ion term, 7F_6 splits into 3 doublets and 7 singlets, but the two lowest lying ones form a quasi doublet, of two levels just separated by 1.4 K [30], while the next level is about 100 K above. The wavefunctions corresponding to the two lowest levels are combinations of $|\pm 6\rangle$ and $|\pm 2\rangle$ but with the major contribution coming from the $J_z = \pm 6$ states. Tb^{3+} behaves as a quasi perfect Ising ion, with FM dipolar interaction. The magnetic moment at low temperature is $\mu = 8.93 \mu_B$, slightly lower than for the free ion, $\mu = 9 \mu_B$. Tb^{3+} orders

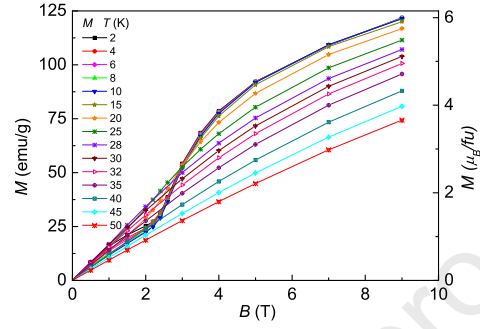


Figure 7: Isothermal magnetization of the scheelite TbCrO_4 in emu/g (left side scale) and in μ_B/fu (right side scale).

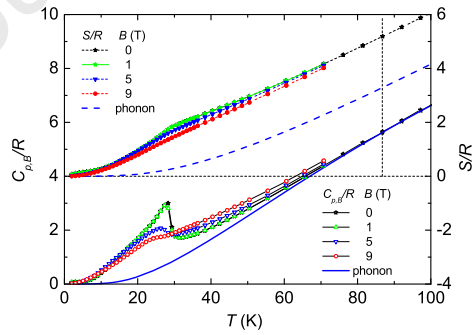


Figure 8: Heat capacity (left side scale) and entropy (right side scale) of the scheelite phase of TbCrO_4 .

345 ferromagnetically at $T_C = 2.86$ K via dipolar interaction [30].

These features can be transferred to some extent to the scheelite TbCrO_4 , where the crystal field splitting is higher. Additionally, the main exchange interaction is Cr^{5+} - Cr^{5+} . This compound has been described as AFM with $T_N = 29$ K and the moments along the c -axis at 2 K [14]. However, below T_N and similarly to the scheelite DyCrO_4 [38], TbCrO_4 undergoes a metamagnetic transition. New magnetization measurements have been done with narrower temperature step (Fig. 7), in order to deduce the MCE via the Maxwell relation. The M -data show a sudden increase at $B_{sf} = 2.6$ T below T_N that can be associated to the spin-flip transition in an Ising system. In a powder sample the jump in M is not discontinuous due to the random orientation of the grains. Consequently, in spite of the metamagnetic transition M does not reach the theoretical saturation value, $M_s \simeq 10\mu_B/fu$, for a high field as 9 T.

The DC molar susceptibility, χ , between T_N and 50 K, follows the Curie-Weiss law, $\chi = C/(T + \theta)$ with $C = 21.60 \mu_B K f u^{-1} T^{-1}$ and $\theta = -3.6$ K. For two different atoms in the formula unit (*i.e.* Cr^{5+} and Tb^{3+}) the Curie constant results $C = N_A \mu_B^2 / (3k_B) \times [g_1^2(s_1(s_1 + 1) + g_2^2 s_2(s_2 + 1))/3]$, where the divisor 3 for the contribution of Tb^{3+} comes from the random grain orientation in a powder sample containing a strongly uniaxial anisotropic ion, and assuming negligible its perpendicular susceptibility. Because for Cr^{5+} , $g_1 = 2$, $s_1 = 1/2$, the contribution of Cr is $0.672 \mu_B K f u^{-1} T^{-1}$. For Tb^{3+} , considering an Ising pseudo-spin $1/2$, $g_2 = 18$, $s_2 = 1/2$ accounts $18.1 \mu_B K f u^{-1} T^{-1}$, the Curie constant is $C = 18.8 \mu_B K f u^{-1} T^{-1}$. This value is similar to the experimental one, but slightly lower since most probably the perpendicular susceptibility is not exactly zero. In any case, the experimental value is far from that for free ions, obtained taking $g_2 = 1.5$ (the Landé factor for the term 7F_6) and $s_2 = J = 6$. Only at temperatures much higher than the crystal-field splitting (*i. e.* at RT or higher) the free ion C values are expected. This departure from the free-ion behavior occurs also in the zircon phase and has important consequences on the MCE (see below).

The heat capacity (Fig. 8) at zero field has a λ -type anomaly at $T_N = 28.2 \pm 0.2$ K, corresponding to an AFM ordering of both magnetic ions, as previously reported from AC susceptibility, heat capacity, and neutron diffraction [13, 14]. At that time there were not reliable data to estimate the phonon contribution and no many conclusions could be extracted from heat capacity. Using precise measurements of C_p in the non-magnetic isostructural LaNbO_4 [25], the magnetic contribution could be deduced. If the CF levels of

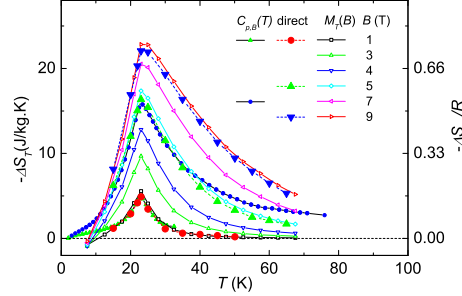


Figure 9: ΔS_T of TbCrO_4 , zircon. Data from heat capacity, from isothermal magnetization and directly measured.

Tb^{3+} in TbLiF_4 would be also considered valid for TbCrO_4 the total magnetic entropy should be $S_m(T \gg T_N)/R = \ln(2) + \ln(2)$, as the sum of the Cr^{5+} and the Tb^{3+} contributions. Actually the experimental entropy (up to 85 K) is $S_m(T \gg T_N)/R = 1.81 \simeq \ln(2) + \ln(3)$. This entropy content indicates that well above T_N there are three populated levels of Tb^{3+} , meaning that a singlet has much lower energy than in TbLiF_4 . Under an applied field of 1 T the peak does not change, as corresponds to an AFM configuration, but under 3 T (Fig. 3 in [14]) or higher it becomes a round anomaly according to the M data, showing a spin-flip transition for 2.6 T.

3.3. Magnetocaloric effect of zircons

The MCE of GdCrO_4 was previously reported [4]. The anisotropy energy of Gd^{3+} is about 1 K, then negligible in the temperature range considered in this work. The exchange interaction $\text{Gd}^{3+}-\text{Cr}^{5+}$ is significantly weaker than the $\text{Cr}^{5+}-\text{Cr}^{5+}$ one, but much stronger than the $\text{Gd}^{3+}-\text{Gd}^{3+}$ one. In such circumstance Gd^{3+} is only weakly polarized by Cr^{5+} at $T_C = 21.3$ K, which leaves room to polarize it by an external field well below T_C , differently of most ferromagnets. As a consequence, GdCrO_4 has strong MCE in a wide temperature range, overcoming 20 J/kg.K between 5 K and 35 K for $B = 9$ T. Taking the data for $B = 5$ T as most frequently reported, the maximum entropy change is $|\Delta S_{T,max}| = 19.0 \text{ J/kg}^{-1}\text{K}^{-1}$ at 22 K.

ΔS_T of TbCrO_4 (Fig. 9) has been deduced in the three ways indicated in section 2.3.1. The results indicate graphically the limitations of each method, although all of them agree near the maximum. In this case the heat capacity

can be extrapolated to $T \rightarrow 0$. Therefore $T_0 = 0$ was taken in eq. (1) and each determination is independent. For $B = 5$ T a moderate maximum value $\Delta S_{T,max} = 16.4$ J kg⁻¹ K⁻¹ is obtained at 23 K. As mentioned above, in the paramagnetic state of TbCrO₄ the JT distortion near 60 K splits the CF quasi-quartet into two quasi-doublets, the higher one being thermally depopulated near T_C . Adding the contribution of Cr⁵⁺ that gives an initial total magnetic entropy $\Delta S_{ini,m}/R \simeq 2 \ln(2) = 1.39$. Correspondingly, this value is an upper bound for the entropy reduction by magnetic field well below 60 K, despite the high magnetic moment of Tb³⁺ ($\mu = 7.6 \mu_B$ [9]), higher than the Gd³⁺ moment, but in any case quite lower than that value for free Tb³⁺, $\mu(\text{free}) = 9 \mu_B$) and the large angular momentum, $J = 6$. If the ideal zircon structure would remain down to very low temperatures the initial entropy of Tb³⁺ would be near $\ln(4)$. Therefore the JT distortion makes the entropy change quite lower than for other $R\text{CrO}_4$ in the zircon phase.

As mentioned before, in HoVO₄, Ho³⁺ behaves as a van Vleck paramagnet [18]. The ground state is not magnetic but the first excited one is a doublet lying only 19.5 cm⁻¹ above. It consist of two states with opposite high magnetic moments and thermally populated near 20 K or above. The magnetic entropy can be deduced from heat capacity data. In the case of HoCrO₄, just above T_C (e.g. $T = 30$ K) the initial magnetic entropy $S(30 \text{ K}, B = 0)/R = 1.74$ and can be understood as a contribution from Cr⁵⁺, close to $\ln(2)$, and another one from Ho³⁺, estimated from experiment as $1.74 - \ln(2) = 1.05$. This value is lower than in HoVO₄ which indicates a higher crystal-field splitting in the Cr compound. For the two-level approximation (neglecting the thermal occupation of higher levels) this entropy corresponds to a splitting around 45 K (31 cm⁻¹), or lower if $S_m(\text{Cr}^{5+})/R < \ln(2)$.

Due to the high moment of the system this relatively high initial entropy can be easily reduced by an external field. Consequently, the MCE (Fig. 10) is stronger than for TbCrO₄, with $|\Delta S_T|$ reaching 30.7 J kg⁻¹ K⁻¹ for $B = 9$ T (or 21.2 J kg⁻¹ K⁻¹ for 5 T), near T_C . The data from heat capacity agree with those deduced from isothermal magnetization [7], especially when the demagnetization factor (lower for the magnetization experiment) is considered. The maximum $|\Delta S_{T,max}|$ overcomes that of GdCrO₄ at the same temperature, but decays much faster below T_C .

Due to the high anisotropy of Ho³⁺, there is another possible and interesting property of HoCrO₄. This compound orders ferromagnetically in the *ab*-plane [9] of the tetragonal zircon structure. The entropy reduction would be strong when the field is applied in that plane, but much smaller when

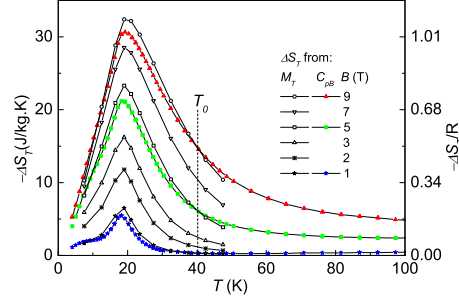


Figure 10: ΔS_T of HoCrO_4 , zircon. Solid symbols: Data from heat capacity. Open symbols: Data from isothermal magnetization. At $T_0 = 40$ K, ΔS_T has been taken from the magnetization data in order to determine the absolute entropy for lower fields.

applied in the c -direction. Therefore a highly anisotropic MCE can be expected in a single crystal. The present results have been obtained in powder, when the random orientation of grains inhibits a complete orientation of the moments along the field. Actually even at 5 K ($T \simeq T_c/4$), in the FM state the saturation is not reached for a so strong field as 8 T. In a single crystal, or in a previously oriented sample by an external field, there would be a strong MCE by a 90° rotation in a constant field. This anisotropy has been invoked as an interesting MCE effect by rotation in a constant field (e. g. in $\text{Dy}(\text{HCOO})_3$ [39]), but usually such systems are pseudo-Ising, with a modest maximum molar entropy change of $R \ln(2)$. In HoCrO_4 the presence of two magnetic atoms and the higher initial entropy of Ho^{3+} would enhance this effect.

ΔS_T of the ErCrO_4 zircon has been deduced from magnetization (Fig. 11). It is similar to that of HoCrO_4 in spite of a quite different CF levels scheme. In ErVO_4 the free-ion manifold of Er^{3+} , $^4I_{15/2}$, splits into 8 Kramers doublets. The first excited doublet is at 43 cm^{-1} [18] and is not thermally populated. It orders AFM at 0.4 K. The close related zircon ErCrO_4 is AFM below $T_N = 15$ K, but the very weak spin-flip field near 0.04 T provokes a parallel alignment of the moments with a stronger field [21]. $|\Delta S_T|$, obtained from isothermal magnetization data, shows a maximum of about 20 J/kg.K at 15 K for a field of 5 T. Dong *et al.* [17] do not report any spin-flip at low temperature and describe the transition at 15 K as FM, although the neutron diffraction experiment [21] shows an AFM spin configuration at 2 K

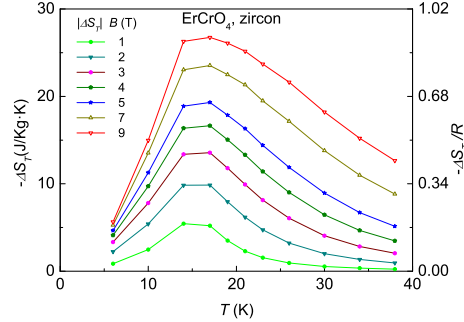


Figure 11: ΔS_T of ErCrO_4 , zircon from magnetization data.

and zero field. Probably the existence of a small spin-flip field or not could be due to the external shape of the sample, via the demagnetizing field. The moment at 5 K, for $B = 5$ T, $\mu = 7 \mu_B/fu$ is largely below the maximum for the free atom ($9 \mu_B$) plus that of Cr^{5+} ($1 \mu_B$), which makes $10 \mu_B$. This behavior in a powder sample seems due to the random orientation of the grains with respect to the external field, along with a strong anisotropy as revealed by the crystal-field splitting of the Er^{3+} ion. In powder, ErCrO_4 has lower MCE than HoCrO_4 , since the ground state is a Kramers doublet (*i. e.* the molar initial entropy of Er^{3+} is only $R \ln(2)$) but it could be more anisotropic and interesting in single crystal due to a strong MCE by rotation in a constant field.

The mean-field calculation given in [17] is made under the assumption that Cr^{5+} and Er^{3+} behave together as an average free ion, with $J = 6$ and $g = 15/14$, which is not physically justified. Actually for a free ion is $L = 6$, $S = 3/2$, $J = 15/2$, $g = 102/85$, which gives the maximum moment of $9 \mu_B$. The fair agreement of the calculated ΔS_T at high temperatures with the experimental data is due to the average over the directions in a powder sample. But the saturation moment in the model is $6 \mu_B/fu$ that is already surpassed by the experimental magnetization data at 2 K with a field of only 3 T, when M is far from saturation.

3.4. Magnetocaloric effect of scheelites.

The scheelites are AFM, which reduces the MCE with respect to zircons. This fact overrides the use as practical refrigerators, but the study of their MCE reveals interesting chemical and physical features. The most intense in-

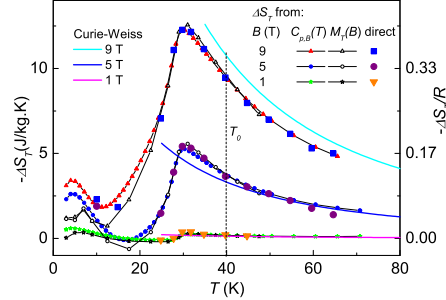
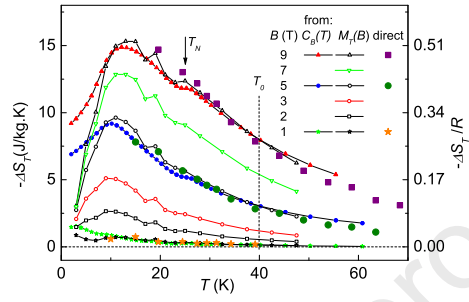
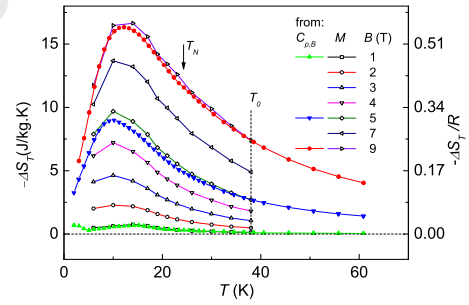


Figure 12: ΔS_T of TbCrO_4 , scheelite. Only three curves are depicted for clarity. Vertical line: Temperature taken to set the entropies with respect to that of 9 T. Dashed lines: Curie-Weiss-like (Eq. 3) curves.

teraction is the AFM Cr^{5+} - Cr^{5+} exchange, as revealed by compounds where the rare earth site is occupied by a non magnetic ion. The MCE depends on the exchange between the R^{3+} and Cr^{5+} . In TbCrO_4 , Tb^{3+} orders simultaneously with Cr^{5+} , as deduced by the heat capacity and isothermal magnetization. Consequently the MCE is conventional for an antiferromagnet. That is, for $T > T_N$ and moderate fields ΔS_T follows a sort of Curie-Weiss law for the entropy [24]

$$\frac{\Delta S_T}{R} \simeq -\frac{[C(\text{Tb})/3 + C(\text{Cr})]B^2}{2R(T + \theta)^2} \quad (3)$$

the Curie constants being $C = N_A \mu_B^2 g^2 s(s+1)/3k_B$, as for susceptibility (section 3.2.3), Tb^{3+} considered as an Ising pseudo-spin, $g = 18$, $s = 1/2$.
 490 The quasi-Ising behavior of the Tb^{3+} ion and the positive value of $\theta \simeq T_N = 25$ K reduces the entropy change in a powder sample with respect to other compounds with lower atomic magnetic moment (Fig. 12). In this sense, even for a single crystal if the field was applied in the easy direction, for high B values ΔS_T is smaller than expected for a free ion Tb^{3+} , although
 495 the magnetic moment is approximately the same. It is so because the lowest manifold term of the free Tb^{3+} is 7F_6 with an initial entropy at zero field $S_m(\text{Tb})/R = \ln J(J+1) = \ln(42) = 3.74$, instead of $\ln(2) = 0.69$. When the field is applied along the easy direction, the magnetization saturates easily above the spin-flip field, that in the case of TbCrO_4 is estimated in 2.6 T
 500 (Fig. 7).

Figure 13: ΔS_T of HoCrO_4 , scheelite phase.Figure 14: ΔS_T of ErCrO_4 , scheelite phase.

Quite differently, in HoCrO_4 (Fig. 13) and ErCrO_4 (Fig. 14) the maximum entropy change for a given field variation occurs well below T_N , which cannot be distinguished in the ΔS_T data for the Er compound and with only
 505 as a small kink in the Ho one. This behavior is very unusual in an antiferromagnet and can be explained if the rare earth is very weakly polarized by the effective exchange field of Cr^{5+} and the contribution of the rare earth to the entropy is not significantly reduced by the AFM ordered Cr^{5+} ions. Consequently, the rare earth behaves in a similar way to a paramagnet. Nevertheless, between 5 K and 50 K, neither Ho^{3+} nor Er^{3+} do not behave as simple Ising systems (the ground doublet in each case). The bump in $C_{p,B}$ near 8 K in both cases indicates that upper levels, mainly the first excited singlet, are thermally populated. Therefore the effect of an external magnetic field on the excited levels, especially the first excited one, cannot be
 510 neglected. In these conditions the contribution of the rare earth to the MCE is much stronger than expected for an antiferromagnet below T_N . Oppositely the unchanged peak in $C_{p,B}$ at T_N indicates that the magnetic field affects weakly to Cr^{5+} below T_N .

4. Conclusions

520 The MCE of the zircon and scheelite phases of $R\text{CrO}_4$ ($R = \text{Tb}, \text{Ho}, \text{Er}$) have been studied in the range 5 K - 100 K. According to the reported data the zircons are ferromagnetic (ErCrO_4 is AF with a very weak spin-flip field) and the scheelites are antiferromagnetic. New data of magnetization and heat capacity have been used to obtain the isothermal entropy increment, ΔS_T , on application of an external magnetic field up to 9 T.
 525

The results can be compared with the previous ones for the zircon GdCrO_4 . In this compound, where Gd^{3+} has no relevant anisotropy in the temperature range of this study, the exchange with Cr^{5+} is moderately weak in such a way that it is not strong enough to polarize Gd^{3+} but helps to an external
 530 field to produce below T_C a much stronger MCE than a paramagnet and a ferromagnet below T_C .

The compounds presented here are in the other extreme of high anisotropy. Speaking about zircon, the Tb compound undergoes a co-operative JT transition near 60 K. The JT transition is reflected by a jump in heat capacity due to the change of the low lying crystal-field levels of Tb^{3+} from a quasi-quartet to two highly spaced quasi-doublets. This fact (*i. e.* the low initial
 535 entropy of a system for only two levels) is the reason for the relatively low

MCE near $T_C = 22$ K, when $|\Delta S_T| = 16.3$ J kg⁻¹ K⁻¹ for $B = 5$ T, despite the high magnetic moment.

540 The scheelite phase of TbCrO₄ does not undergo a JT transition. Since the electrostatic interaction Tb³⁺-O²⁻ is stronger than Tb³⁺-F⁻, in the scheelite TbLiF₄ most probably there are several CF levels thermally populated near $T_N = 29$ K. Due to the relatively strong exchange coupling between Cr⁵⁺ and Tb³⁺ and the high moment of Tb³⁺ the spin-flip field is relatively
545 low and the MCE has the typical features of an antiferromagnet.

In the zircon phase the MCE of HoCrO₄ looks like in a conventional ferromagnet, with a high maximum just above $T_C = 17$ K. The lowest crystal field levels are a non-magnetic singlet and one doublet nearly above. That allows a relatively high initial entropy at T_C . Consequently the MCE is
550 strong near T_C with $|\Delta S_T| = 30.7$ J/kg.K, but decays quickly below, when the only populated state at zero field is the singlet. The MCE of the zircon ErCrO₄ shows similar features to ErCrO₄, although the CF splitting scheme is different.

In the scheelite phase Ho and Er compounds behave also similarly. The
555 R^{3+} -Cr⁵⁺ exchange coupling seems much weaker than in the Gd compound. Extrapolating from $RLiF_4$ scheelites, the lowest CF states are two Kramers doublets for Er³⁺ and a non-Kramers doublet and a singlet for Ho³⁺. In both cases the heat capacity has a Schottky-like anomaly due to the thermal population of these levels. Due to the weak R^{3+} -Cr⁵⁺ coupling the MCE
560 seems to that a paramagnet. Strikingly, $|\Delta S_T|$ is much higher below T_N , where probably only Cr⁵⁺ is substantially ordered.

Acknowledgments

This work has been funded by Spanish MINECO and FEDER (Projects MAT2017-86019-R and MAT2017-84385-R), Gobierno de Aragón (Consolidated Group E100). Authors would like to acknowledge the use of the
565 Servicio General de Apoyo a la Investigación-SAI, Universidad de Zaragoza.

- [1] W. F. Giaque, D. P. MacDougall, Attainment of temperatures below 1° absolute by demagnetization of Gd₂(SO₄)₃·8H₂O, Phys. Rev. 43 (1933) 768–768. doi:10.1103/PhysRev.43.768.
570 URL <https://link.aps.org/doi/10.1103/PhysRev.43.768>
- [2] P. J. Shirron, Applications of the magnetocaloric effect in single-stage, multi-stage and continuous adiabatic de-

- magnetization refrigerators, *Cryogenics* 62 (2014) 130–139.
doi:<https://doi.org/10.1016/j.cryogenics.2014.03.014>.
575 URL <https://www.sciencedirect.com/science/article/pii/S0011227514000654>
- [3] H. Zhang, R. Gimaev, B. Kovalev, K. Kamilov, V. Zverev, A. Tishin, Review on the materials and devices for magnetic refrigeration in the temperature range of nitrogen and hydrogen liquefaction, *Physica B: Condensed Matter* 558 (2019) 65–73.
580 doi:<https://doi.org/10.1016/j.physb.2019.01.035>.
URL <https://www.sciencedirect.com/science/article/pii/S0921452619300316>
- [4] E. Palacios, C. Tomasi, R. Sáez-Puche, A. J. Dos santos García, F. Fernández-Martínez, R. Burriel, Effect of Gd polarization on the large magnetocaloric effect of GdCrO_4 in a broad temperature range,
585 *Phys. Rev. B* 93 (2016) 064420. doi:10.1103/PhysRevB.93.064420.
URL <https://link.aps.org/doi/10.1103/PhysRevB.93.064420>
- [5] E. Palacios, C. Tomasi, R. Saez-Puche, A. J. dos Santos-Garcia, F. Fernandez-Martinez, R. Burriel, Enhanced magnetocaloric effect by the rare earth polarization due to the exchange with a transition metal
590 - study of GdCrO_4 , in: *Solid Compounds of Transition Elements*, Vol. 257 of *Solid State Phenomena*, Trans Tech Publications Ltd, 2017, pp. 139–142. doi:10.4028/www.scientific.net/SSP.257.139.
- [6] E. Jimenez-Melero, P. Gubbens, M. Steenvoorden, S. Sakarya, A. Goosens, P. D. De Réotier, A. Yaouanc, J. Rodríguez-Carvajal, B. Be-
595 uneu, J. Isasi, et al., A combined study of the magnetic properties of GdCrO_4 , *Journal of Physics: Condensed Matter* 18 (34) (2006) 7893.
doi:<https://doi.org/10.1088/0953-8984/18/34/004>.
- [7] A. Midya, N. Khan, D. Bhoi, P. Mandal, 3d-4f spin interaction induced giant magnetocaloric effect in zircon-type DyCrO_4 and
600 HoCrO_4 compounds, *Applied Physics Letters* 103 (9) (2013) 092402.
doi:10.1063/1.4819768.
- [8] E. Jiménez, J. Isasi, R. Sáez-Puche, Synthesis, structural characterization and magnetic properties of $R\text{CrO}_4$ oxides, $R = \text{Nd}, \text{Sm}, \text{Eu}$ and Lu , *Journal of Alloys and Compounds* 312 (1) (2000) 53–59.
605 doi:[https://doi.org/10.1016/S0925-8388\(00\)01079-3](https://doi.org/10.1016/S0925-8388(00)01079-3).
URL <https://www.sciencedirect.com/science/article/pii/S0925838800010793>

- [9] E. Jiménez-Melero, Estudio cristalográfico y magnético de óxidos $R\text{CrO}_4$ ($R =$ tierra rara), Ph.D. thesis, Facultad de Ciencias Químicas (2005). URL <https://eprints.ucm.es/id/eprint/7130/>
- 610 [10] K. Tezuka, Y. Doi, Y. Hinatsu, Crystal structures and magnetic properties of zircon-type compounds $\text{Lu}_1-x\text{Y}_x\text{CrO}_4$, Journal of Materials Chemistry 12 (4) (2002) 1189–1193. doi:10.1039/B108483F.
- [11] R. Sáez-Puche, E. Jiménez, J. Isasi, M. T. Fernández-Dáz, J. L. García-Muoz, Structural and magnetic characterization of $R\text{CrO}_4$ oxides ($R =$ Nd, Er and Tm), Journal of Solid State Chemistry 171 (1) (2003) 161–169, proceedings from the 23rd Rare Earth Research Conference UC Davis Campus, July 13-16, 2002. doi:[https://doi.org/10.1016/S0022-4596\(02\)00203-7](https://doi.org/10.1016/S0022-4596(02)00203-7). URL <https://www.sciencedirect.com/science/article/pii/S0022459602002037>
- 620 [12] E. Climent-Pascual, J. Romero de Paz, J. M. Gallardo-Amores, R. Sez-Puche, Ferromagnetism vs. antiferromagnetism of the dimorphic HoCrO_4 oxide, Solid State Sciences 9 (7) (2007) 574–579, bordeaux June 2006. doi:<https://doi.org/10.1016/j.solidstatesciences.2007.03.003>. URL <https://www.sciencedirect.com/science/article/pii/S1293255807000441>
- 625 [13] E. Climent, J. Gallardo, J. R. de Paz, N. Taira, R. S. Puche, Phase transition induced by pressure in TbCrO_4 oxide: Relationship structureproperties, Journal of Alloys and Compounds 488 (2) (2009) 524–527, proceedings of the 25th Rare Earth Research Conference, June 22-26, Tuscaloosa, Alabama, USA. doi:<https://doi.org/10.1016/j.jallcom.2008.10.060>. URL <https://www.sciencedirect.com/science/article/pii/S0925838808017155>
- 630 [14] E. Climent Pascual, J. M. Gallardo Amores, R. Sáez Puche, M. Castro, N. Taira, J. Romero de Paz, L. C. Chapon, Zircon to scheelite phase transition induced by pressure and magnetism in TbCrO_4 , Phys. Rev. B 81 (2010) 174419. doi:10.1103/PhysRevB.81.174419. URL <https://link.aps.org/doi/10.1103/PhysRevB.81.174419>
- 635 [15] A. Dos santos-García, E. Climent-Pascual, J. Gallardo-Amores, M. G. Rabie, Y. Doi, J. Romero de Paz, B. Beuneu, R. Sáez-Puche, Synthesis and magnetic properties of the high-pressure scheelite-type GdCrO_4 polymorph, Journal of Solid State Chemistry 194 (2012) 119–126.
- 640

doi:<https://doi.org/10.1016/j.jssc.2012.04.044>.

URL <https://www.sciencedirect.com/science/article/pii/S0022459612003052>

- [16] M. S. Rabie, Pressure-induced phase transitions in $R\text{CrO}_4$ oxides: preparation, magnetic and electronic properties (R = rare earth, Ph.D. thesis, Facultad de Ciencias Químicas (2013).
645 URL <https://eprints.ucm.es/id/eprint/21669/>
- [17] Q. Dong, Y. Ma, Y. Ke, X. Zhang, L. Wang, B. Shen, J. Sun, Z. Cheng, Ericsson-like giant magnetocaloric effect in $\text{GdCrO}_4\text{ErCrO}_4$ composite oxides near liquid hydrogen temperature, *Materials Letters* 161 (2015) 669–673. doi:<https://doi.org/10.1016/j.matlet.2015.09.070>.
650 URL <https://www.sciencedirect.com/science/article/pii/S0167577X15305784>
- [18] G. J. Bowden, A review of the low temperature properties of the rare earth vanadates, *Australian Journal of Physics* 51 (1998) 201–236.
URL <https://www.publish.csiro.au/PH/pdf/P97066>
- [19] E. Palacios, J. A. Rodríguez-Velamazán, M. Evangelisti, G. J. McIntyre, G. Lorusso, D. Visser, L. J. de Jongh, L. A. Boatner, Magnetic structure and magnetocalorics of GdPO_4 , *Phys. Rev. B* 90 (2014) 214423. doi:10.1103/PhysRevB.90.214423.
655 URL <https://link.aps.org/doi/10.1103/PhysRevB.90.214423>
- [20] A. Indra, K. Dey, J. K. Dey, S. Majumdar, U. Rütt, O. Gutowski, M. v. Zimmermann, S. Giri, cro_4 distortion-driven ferroelectric order in $(r, Y)\text{cro}_4$ ($r = \text{Sm, Gd, and Ho}$): A new family of multiferroics, *Phys. Rev. B* 98 (2018) 014408. doi:10.1103/PhysRevB.98.014408.
660 URL <https://link.aps.org/doi/10.1103/PhysRevB.98.014408>
- [21] E. Jiménez, J. Isasi, M. T. Fernández, R. Sáez-Puche, Magnetic behavior of ercro_4 oxide, *Journal of Alloys and Compounds* 344 (1) (2002) 369–374, proceedings of the Rare Earths‘ 2001 Conference. doi:[https://doi.org/10.1016/S0925-8388\(02\)00387-0](https://doi.org/10.1016/S0925-8388(02)00387-0).
665 URL <https://www.sciencedirect.com/science/article/pii/S0925838802003870>
- [22] E. Jiménez, W. Kraan, N. van Dijk, P. Gubbens, J. Isasi, R. Sáez-Puche, Magnetic domains in ercro_4 studied by 3d neutron depolarization, *Physica B: Condensed Matter* 350 (1, Supplement) (2004) E293–E296, proceedings of the Third European Conference on Neutron Scattering.
670

- doi:<https://doi.org/10.1016/j.physb.2004.03.073>.
675 URL <https://www.sciencedirect.com/science/article/pii/S0921452604002509>
- [23] R. Sáez-Puche, E. Climent, M. G. Rabie, J. Romero, J. M. Gallardo, Neutron diffraction characterization and magnetic properties of the scheelite-type ErCrO_4 polymorph, *Journal of Physics: Conference Series* 325 (2011) 012012. doi:10.1088/1742-6596/325/1/012012.
680 URL <https://doi.org/10.1088/1742-6596/325/1/012012>
- [24] E. Palacios, M. Evangelisti, R. Sáez-Puche, A. J. Dos Santos-García, F. Fernández-Martínez, C. Cascales, M. Castro, R. Burriel, O. Fabelo, J. A. Rodríguez-Velamazán, Magnetic structures and magnetocaloric effect in $R\text{VO}_4$ ($R = \text{Gd}, \text{Nd}$), *Phys. Rev. B* 97 (2018) 214401. doi:10.1103/PhysRevB.97.214401.
685 URL <https://link.aps.org/doi/10.1103/PhysRevB.97.214401>
- [25] G. Nikiforova, A. Khoroshilov, A. Tyurin, V. Gurevich, K. Gavrichev, Heat capacity and thermodynamic properties of lanthanum orthoniobate, *The Journal of Chemical Thermodynamics* 132 (2019) 44–53. doi:<https://doi.org/10.1016/j.jct.2018.12.041>.
690 URL <https://www.sciencedirect.com/science/article/pii/S0021961418308875>
- [26] C.-G. Li, X.-Y. Kuang, R.-P. Chai, Y.-R. Zhao, The defect structure and EPR parameters for Er^{3+} in molybdates: a complete energy matrices study, *Molecular Physics* 110 (24) (2012) 3023–3029. arXiv:<https://doi.org/10.1080/00268976.2012.695026>, doi:10.1080/00268976.2012.695026.
695 URL <https://doi.org/10.1080/00268976.2012.695026>
- [27] Vishwamittar, S. Taneja, S. Puri, On the behaviour of Er^{3+} ion in tetragonal crystalline fields, *Journal of Physics and Chemistry of Solids* 33 (5) (1972) 965–971. doi:[https://doi.org/10.1016/S0022-3697\(72\)80256-7](https://doi.org/10.1016/S0022-3697(72)80256-7).
700 URL <https://www.sciencedirect.com/science/article/pii/S0022369772802567>
- [28] P. E. Hansen, T. Johansson, R. Nevald, Magnetic properties of lithium rare-earth fluorides: Ferromagnetism in LiErF_4 and LiHoF_4 and crystal-field parameters at the rare-earth and Li sites, *Phys. Rev. B* 12 (1975) 5315–5324. doi:10.1103/PhysRevB.12.5315.
705 URL <https://link.aps.org/doi/10.1103/PhysRevB.12.5315>

- [29] H. P. Christensen, Spectroscopic analysis of LiHoF_4 and LiHoF_4 , Phys. Rev. B 19 (1979) 6564–6572. doi:10.1103/PhysRevB.19.6564.
710 URL <https://link.aps.org/doi/10.1103/PhysRevB.19.6564>
- [30] J. Magariño, J. Tuchendler, P. Beauvillain, I. Laursen, EPR experiments in LiTbF_4 , LiHoF_4 , and LiErF_4 at submillimeter frequencies, Phys. Rev. B 21 (1980) 18–28. doi:10.1103/PhysRevB.21.18.
URL <https://link.aps.org/doi/10.1103/PhysRevB.21.18>
- 715 [31] I. V. Romanova, A. V. Egorov, S. L. Korableva, B. Z. Malkin, M. S. Tagirov, 19f NMR study of LiTbF_4 single crystals, Journal of Physics: Conference Series 324 (2011) 012034. doi:10.1088/1742-6596/324/1/012034.
URL <https://doi.org/10.1088/1742-6596/324/1/012034>
- 720 [32] P. Babkevich, A. Finco, M. Jeong, B. D. Piazza, I. Kovacevic, G. Klughertz, K. W. Kramer, C. Kraemer, D. T. Adroja, E. Goremychkin, T. Unruh, T. Strässle, A. D. Lieto, J. Jensen, H. M. Rønnow, Neutron spectroscopic study of crystal-field excitations and the effect of the crystal field on dipolar magnetism in LiRF_4 ($R = \text{Gd, Ho, Er, Tm, and Yb}$), Physical Review B 92 (2015) 144422. doi:10.1103/PhysRevB.92.144422.
725
- [33] E. Palacios, R. Sez-Puche, J. Romero, Y. Doi, Y. Hinatsu, M. Evangelisti, Large magnetocaloric effect in EuGd_2O_4 and EuDy_2O_4 , Journal of Alloys and Compounds 890 (2022) 161847. doi:<https://doi.org/10.1016/j.jallcom.2021.161847>.
730 URL <https://www.sciencedirect.com/science/article/pii/S0925838821032564>
- [34] G. Buisson, F. Tchéou, F. Sayetat, K. Scheunemann, Crystallographic and magnetic properties of TbCrO_4 at low temperature (x-ray and neutron experiments), Solid State Communications 18 (7) (1976) 871–875. doi:[https://doi.org/10.1016/0038-1098\(76\)90226-X](https://doi.org/10.1016/0038-1098(76)90226-X).
735 URL <https://www.sciencedirect.com/science/article/pii/003810987690226X>
- [35] M. Wells, R. Worswick, The specific heat of terbium vanadate TbVO_4 , Physics Letters A 42 (4) (1972) 269–270. doi:[https://doi.org/10.1016/0375-9601\(72\)90416-1](https://doi.org/10.1016/0375-9601(72)90416-1).
740 URL <https://www.sciencedirect.com/science/article/pii/0375960172904161>

- [36] G. A. Gehring, K. A. Gehring, Co-operative jahn-teller effects, Reports on Progress in Physics 38 (1) (1975) 1–89. doi:10.1088/0034-4885/38/1/001.
URL <https://doi.org/10.1088/0034-4885/38/1/001>
- 745 [37] S. Skanthakumar, C.-K. Loong, L. Soderholm, M. M. Abraham, L. A. Boatner, Crystal-field excitations and magnetic properties of Ho^{3+} in HoVO_4 , Phys. Rev. B 51 (1995) 12451–12457. doi:10.1103/PhysRevB.51.12451.
URL <https://link.aps.org/doi/10.1103/PhysRevB.51.12451>
- 750 [38] Y. Long, Q. Liu, Y. Lv, R. Yu, C. Jin, Various $3d-4f$ spin interactions and field-induced metamagnetism in the Cr^{5+} system DyCrO_4 , Phys. Rev. B 83 (2011) 024416. doi:10.1103/PhysRevB.83.024416.
URL <https://link.aps.org/doi/10.1103/PhysRevB.83.024416>
- 755 [39] G. Lorusso, O. Roubeau, M. Evangelisti, Rotating magnetocaloric effect in an anisotropic molecular dimer, Angewandte Chemie International Edition 55 (2016) n/a–n/a. doi:10.1002/anie.201510468.

Highlights

Zircon to scheelite $R\text{CrO}_4$ ($R = \text{Tb}, \text{Ho}, \text{Er}$) phase transition induced at high pressure and high temperature.

Magnetic measurements reveal that $R\text{CrO}_4$ Zircons behave as ferromagnetic while the $R\text{CrO}_4$ Scheelites are antiferromagnetic.

Heat capacity, magnetization and direct calorimetric measurements had been done in order to determine the magnetic entropy variation for both zircon and scheelite $R\text{CrO}_4$ oxides.

Zircon $R\text{CrO}_4$ phases show large magnetocaloric effect according to their ferromagnetic behavior. This effect appear to be lower than in the case of scheelite polymorphs.

Zircon RCrO_4 phases show large magnetocaloric effect according to their ferromagnetic behavior. This effect as it is expected is lower in the case of antiferromagnetic scheelite polymorphs.

Journal Pre-proof

Highligts

Zircon to scheelite RCrO_4 (R= Tb, Ho, Er) phase transition induced at high pressure and high temperature.

Magnetic measurements reveal that RCrO_4 Zircons behave as ferromagnetic while the RCrO_4 Scheelites are antiferromagnetic.

Heat capacity, magnetization and direct calorimetric measurements had been done in order to determine the magnetic entropy variation for both zircon and scheelite RCrO_4 oxides.

Zircon RCrO_4 phases show large magnetocaloric effect according to their ferromagnetic behavior. This effect appear to be lower than in the case of scheelite polymorphs.

Declaration of interests

The authors declare that they have no known competing financial interests or personal relationships that could have appeared to influence the work reported in this paper.

The authors declare the following financial interests/personal relationships which may be considered as potential competing interests:

Journal Pre-proof